Discrimination of Shot-Noise-Driven Poisson Processes by External Dead Time: Application to Radioluminescence from Glass

BAHAA E. A. SALEH, MEMBER, IEEE, JOSEPH T. TAVOLACCI, MEMBER, IEEE, AND MALVIN CARL TEICH, SENIOR MEMBER, IEEE

Abstract—The shot-noise-driven doubly stochastic Poisson point process (SNDP) describes the photodetection statistics for several kinds of luminescence radiation (e.g., cathodoluminescence). This process, which is bunched (clustered) in character and is associated with multiplied Poisson noise, has many applications in pulse, particle, and photon detection. In this work we describe ways in which dead time can be used to constructively enhance or diminish the effects of point processes that display such bunching, according to whether they are signal or noise. We discuss in some detail the subtle interrelations between photocount bunching arising in the SNDP and the antibunching character arising from dead-time effects. We demonstrate that the dead-time-modified count mean and variance for an arbitrary doubly stochastic Poisson point process (DSPP) can be obtained from the Laplace transform of the single-fold and joint moment-generating functions for the driving rate process. The dead time is assumed to be small in comparison with the correlation time of the driving process. Specific calculations have been carried out for the SNDP. The theoretical counting efficiency ϵ_m and normalized variance ϵ_v for shot-noise light with a rectangular impulse response function are shown to depend principally on the dead-time parameter and on the number of primary events in a correlation time of the driving rate process. The values of ϵ_m and ϵ_v are significantly reduced below those obtained with the constant-rate Poisson because of the clustering associated with the SNDP. The theory is in good accord with the experimental values of these quantities for radioluminescence radiation in three transparent materials (fused silica, quartz, and glass). Various parameter values for each material have been extracted. For large counting times, the experimental photon-counting distributions are shown to be well described by the Neyman Type-A theoretical distribution, both in the absence and in the presence of dead time.

Manuscript received July 16, 1981. This work was supported by the Joint Services Electronics Program (U.S. Army, U.S. Navy, and U.S. Air Force) under Contract DAAG29-79-C-0079, by the National Science Foundation under Grant ENG78-26498, and by the Jet Propulsion Laboratory, California Institute of Technology, under Contracts 955335 and 955336 to the Bendix Corporation.

B.E.A. Saleh is with the Columbia Radiation Laboratory, Department of Electrical Engineering, Columbia University, New York, NY 10027, and with the Department of Electrical and Computer Engineering, University of Wisconsin, Madison, WI 53706.

J. T. Tavolacci is with the Guidance Systems Division, Bendix Corporation, Teterboro, NJ 07608.

M. C. Teich is with the Columbia Radiation Laboratory, Department of Electrical Engineering, Columbia University, New York, NY 10027. Portions of this work were carried out under a consultancy arrangement with Guidance Systems Division, Bendix Corporation, Teterboro, NJ 07608.

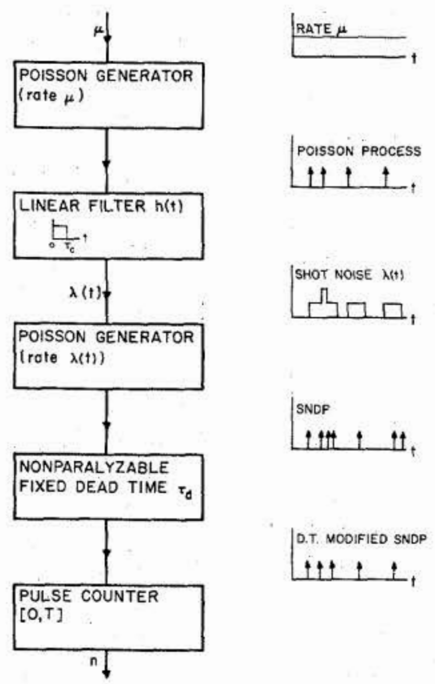

Fig. 1. Block diagram for the generation of a dead-time-modified SNDP.

I. Introduction

THE shot-noise-driven doubly stochastic Poisson point process (SNDP) has been shown to have a broad variety of applications in pulse, particle, and photon detection [1]-[3]. It arises when events of a primary homogeneous Poisson process are filtered, producing a continuous shot-noise process, which in turn acts as the random rate of a secondary Poisson point process (see Fig. 1). It is a doubly stochastic Poisson point process (DSPP). Since events of the secondary point process cluster about events of the primary process, the SNDP is more strongly affected by the presence of dead time than is the homogeneous Poisson process. This property may be exploited to distinguish between an SNDP and a homogeneous (ordinary) Poisson process.

0018-9197/81/1200-2341$00.75

In the present work, we delineate some of the subtle interrelations between photon bunching arising in the SNDP and the antibunching character arising from dead-time effects. In a preliminary manner, we explore ways in which dead time can be used to constructively enhance or diminish the effects of point processes that display bunching, according to whether they are signal or noise.

The problem proves to be rather difficult from a mathematical point of view. Fortunately we are able to make use of general expressions that were recently obtained for the mean and variance of the number of events in a fixed but arbitrary sampling time for an arbitrary DSPP affected by nonparalyzable dead time [4]. In obtaining these expressions, the dead time was assumed to be small in comparison with the characteristic fluctuation time of the driving rate process. The mean was shown to depend only on the first-order statistics of the rate, whereas the variance was formally shown to depend on both the first- and second-order statistics of the rate. The general expressions turned out to be quite complex but could, nevertheless, be evaluated for chaotic light with the help of a great deal of algebra; indeed, an explicit expression was obtained for the dependence of the dead-time-modified variance on the power spectrum of the radiation.

We show here that a Laplace transformation of the singlefold and joint moment-generating functions for the driving rate process provides a ready solution for the dead-time-modified count mean and variance (Section II). Thus, the joint probability density function for the rate process, which is often unknown or quite complex, is not required for the calculation of the variance. Since this result is applicable for an arbitrary DSPP we are able to determine the effect of dead time on the SNDP count mean and variance (Section III). We demonstrate that dead time does indeed reduce the mean and variance more severely, and more selectively, than in the Poisson case.

We have previously shown [1], [2] that photoelectrons generated by radioluminescence radiation may be described by an SNDP. In Section IV, we present experimental photon-counting distributions for radioluminescence radiation induced in three transparent materials (fused silica, quartz, and glass), both in the absence and in the presence of fixed nonparalyzable dead time. The Neyman Type-A theoretical counting distribution, which is obtained as a special case of the SNDP, is shown to provide a very good fit to the data over a substantial range of dead-time values. Finally, the theoretical results derived in Section III are shown to be in accord with the experimental normalized count mean and variance observed at the output of the dead-time-modified photon counter, when the fixed dead time is varied parametrically (Section V). The conclusion is presented in Section VI.

II. Dead-Time-Modified Mean and Variance for an Arbitrary DSPP

In accordance with the results provided by Vannucci and Teich [4], [5], the dead-time-modified mean $E(n)$ and variance $\mathrm{Var}(n)$ for an arbitrary DSPP, driven by a stationary stochastic rate process $\lambda(t)$, are given approximately by

$$E(n) \approx \left\langle \frac{\lambda(t)}{1+\lambda(t)\tau_d} \right\rangle T \tag{1}$$

and

$$\mathrm{Var}(n) \approx \left\langle \frac{\lambda(t)}{(1+\lambda(t)\tau_d)^3} \right\rangle T - \left\langle \frac{\lambda(t)}{1+\lambda(t)\tau_d} \right\rangle^2 T^2 + 2\int_0^T (T-\tau) \left\langle \frac{\lambda(0)}{1+\lambda(0)\tau_d} \cdot \frac{\lambda(\tau)}{1+\lambda(\tau)\tau_d} \right\rangle d\tau. \tag{2}$$

Here τ_d is the dead time, T is the counting time, and the angular brackets $\langle\cdot\rangle$ represent an ensemble average over the statistics of $\lambda(t)$. For the validity of (1), the condition

$$\tau_d \ll \tau_c, \tag{3}$$

where τ_c is the correlation time of the random process $\lambda(t)$, must be satisfied. For the validity of (2), condition (3) must be satisfied, along with the condition

$$\tfrac{1}{6}(\bar{\lambda}\tau_d)^2\,\tau_d \ll \tau_c \tag{4}$$

where $\bar{\lambda}$ is the average value of the rate. Comparing (3) and (4) it is apparent that (4) is less restrictive when $\bar{\lambda}\tau_d < \sqrt{6}$ and more restrictive when $\bar{\lambda}\tau_d > \sqrt{6}$. No constraints on the sampling time are imposed. The case considered is that for which the counter is always connected to the input process; this is the equilibrium counter as opposed to the blocked or unblocked counter. Actually, in the limits where our results are applicable, the number of pulses recorded during a sampling time is $\gg 1$, and therefore the differences among blocked, unblocked, and equilibrium counters become negligible, so that our results are indeed valid for all three types of counters.

We now compute the ensemble averages represented in (1) and (2). If X is a random variable with moment-generating function (mgf) $Q_X(s) = \langle \exp(-sX)\rangle$, then

$$\left\langle \frac{X}{1+X} \right\rangle = 1 - F(1) \tag{5}$$

and

$$\left\langle \frac{X}{(1+X)^3} \right\rangle = -\frac{1}{2}F''(1) - F'(1) \tag{6}$$

where

$$F(u) = \int_0^\infty e^{-us} Q_X(s)\, ds \tag{7}$$

is the Laplace transform of the mgf, and

$$F'(u) = \frac{d}{du}F(u), \qquad F''(u) = \frac{d^2}{du^2}F(u). \tag{8}$$

Also, if X_1 and X_2 are random variables with joint mgf

$$Q_{X_1,X_2}(s_1,s_2) = \langle \exp(-s_1X_1 - s_2X_2)\rangle,$$

then

$$\left\langle \frac{X_1}{1+X_1} \cdot \frac{X_2}{1+X_2} \right\rangle = 1 - 2F(1) + F(1,1) \tag{9}$$

where

$$F(u_1,u_2) = \int_0^\infty \int_0^\infty \exp(-u_1s_1 - u_2s_2) \cdot Q_{X_1,X_2}(s_1,s_2)\, ds_1\, ds_2 \tag{10}$$

is the 2-D Laplace transform of $Q(s_1, s_2)$. The above relations are proved in the Appendix.

With the substitution $X = \lambda$, the straightforward use of these formulas in (1) and (2) results in

$$E(n) = \frac{T}{\tau_d}\left[1 - \frac{1}{\tau_d} F\left(\frac{1}{\tau_d}\right)\right] \tag{11}$$

and

$$\mathrm{Var}\,(n) = -\frac{T}{\tau_d^3} F'\left(\frac{1}{\tau_d}\right) - \frac{T}{2\tau_d^4} F''\left(\frac{1}{\tau_d}\right) - \left[\frac{T}{\tau_d^2} F\left(\frac{1}{\tau_d}\right)\right]^2 + \frac{2}{\tau_d^4}\int_0^T (T-\tau) F\left(\frac{1}{\tau_d}, \frac{1}{\tau_d}, \tau\right) d\tau \tag{12}$$

where $F(u)$ is the Laplace transform of

$$Q_{\lambda(t)}(s) = \langle \exp\,[-s\lambda(t)]\rangle \tag{13}$$

and $F(u_1, u_2, \tau)$ is the 2-D Laplace transform of

$$Q_{\lambda(0),\lambda(\tau)}(s_1, s_2) = \langle \exp\,[-s_1\lambda(0) - s_2\lambda(\tau)]\rangle. \tag{14}$$

Once the single- and two-fold mgf's of $\lambda(t)$ are known, the dead-time-modified mean and variance can be computed from (7), (8), and (10)-(12).

The simplest example is that of deterministic $\lambda(t) = \lambda_0$, in which case

$$Q_{\lambda(t)}(s) = \exp\,(-s\lambda_0) \tag{15}$$

and

$$Q_{\lambda(0),\lambda(\tau)}(s_1, s_2) = \exp\,(-s_1\lambda_0)\exp\,(-s_2\lambda_0). \tag{16}$$

Our formulas then reproduce the known expressions for the dead-time-modified count mean and variance for the Poisson, viz. [6], [7]

$$E(n) \approx \frac{\lambda_0 T}{1 + \lambda_0\tau_d} \tag{17}$$

and

$$\mathrm{Var}\,(n) \approx \frac{\lambda_0 T}{(1 + \lambda_0\tau_d)^3}. \tag{18}$$

For $\lambda(t)$ corresponding to the intensity of chaotic light, we reproduce the formulas previously obtained by Vannucci and Teich [4].

III. Dead-Time-Modified Mean and Variance for the SNDP with Rectangular Impulse-Response Function

We now consider a driving rate $\lambda(t)$ that is a shot-noise process, obtained by passing a homogeneous Poisson point process of rate μ through a rectangular filter of impulse response

$$h(t) = \begin{cases} \alpha/\tau_c & 0 \leqslant t \leqslant \tau_c \\ 0 & \text{elsewhere.}\end{cases} \tag{19}$$

Then [1], [3]

$$Q_{\lambda(t)}(s) = \exp\,\{c(e^{-\beta s} - 1)\} \tag{20}$$

and

$$Q_{\lambda(0),\lambda(\tau)}(s_1, s_2) = \begin{cases} \exp\,\{\mu[(e^{-\beta s_1} - 1)\tau + (e^{-\beta s_2} - 1)\tau \\ \quad + (e^{-\beta s_1 - \beta s_2} - 1)(\tau_c - \tau)]\}, & \tau \leqslant \tau_c, \\ \exp\,\{c(e^{-\beta s_1} - 1)\}\exp\,\{c(e^{-\beta s_2} - 1)\}, & \tau \geqslant \tau_c, \end{cases} \tag{21}$$

where

$$c = \mu\tau_c, \qquad \beta = \alpha/\tau_c. \tag{22}$$

Using (7) and (10), the corresponding Laplace transforms are

$$F(u) = e^{-c}\sum_{k=0}^{\infty}\frac{c^k}{k!(u + \beta k)} \tag{23}$$

and

$$F(u_1, u_2, \tau) = \begin{cases} \displaystyle\sum_{k=0}^{\infty}\sum_{l=0}^{k}\sum_{m=0}^{l}\frac{e^{-c}e^{-\mu\tau}(\mu\tau)^l(c-\mu\tau)^{k-l}}{(k-l)!(l-m)!\,m!\,[u_1 + \beta(k-l+m)]\,[u_2 + \beta(k-m)]}, & \tau \leqslant \tau_c \\ F(u_1)F(u_2), & \tau \geqslant \tau_c. \end{cases} \tag{24}$$

Substitution in (11) and (12) yields the counting efficiency (normalized mean)

$$\epsilon_m = E(n)/\overline{\lambda}T = 1/\overline{\lambda}\tau_d - \nu_1, \tag{25}$$

the ratio of variance to unmodified mean

$$\mathrm{Var}\,(n)/\overline{\lambda}T = \nu_2 - \nu_3 - \overline{\lambda}T\nu_1^2 + w, \tag{26}$$

and the normalized count variance (ratio of variance in the presence of dead time to variance in the absence of dead time)

$$\epsilon_v = \mathrm{Var}\,(n)/(1 + a_1)\overline{\lambda}T. \tag{27}$$

The quantity $\overline{\lambda}T = \mu\alpha T$ is the mean count in the absence of dead time, $a_1 = \alpha/\mathfrak{M}$ where $\mathfrak{M}$ is the number of degrees of freedom of the counting time within the correlation time τ_c of the shot-noise light [1], [2], and $\overline{\lambda}\tau_d = \mu\alpha\tau_d$. Also

$$\nu_m = \frac{1}{\overline{\lambda}\tau_d}e^{-c}\sum_{k=0}^{\infty}\frac{c^{k+m}}{k!(c + \overline{\lambda}\tau_d k)^m}, \qquad m = 1, 2, 3 \tag{28}$$

$$w = \begin{cases} \dfrac{2\alpha}{(\overline{\lambda}\tau_d)^2}e^{-c}\phi(\Gamma c), & \Gamma \leqslant 1 \\ \dfrac{2\alpha}{(\overline{\lambda}\tau_d)^2}e^{-c}\phi(c) + \overline{\lambda}T\left(1 - \dfrac{1}{\Gamma}\right)^2\nu_1^2, & \Gamma \geqslant 1 \end{cases} \tag{29}$$

with

$$\Gamma = T/\tau_c \tag{30}$$

and

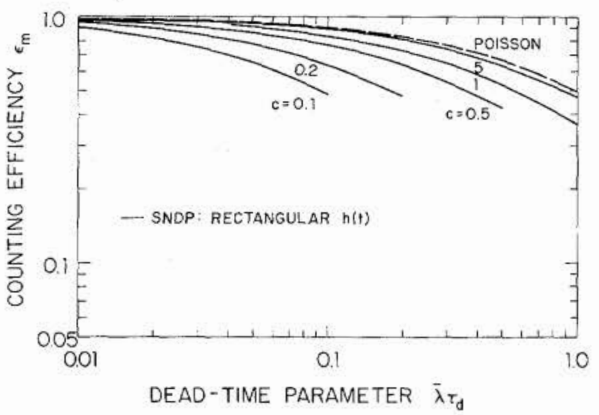

Fig. 2. Counting efficiency $\epsilon_m = E(n)/\bar{\lambda}T$ versus $\bar{\lambda}\tau_d$, where $\bar{\lambda} = \mu\alpha$ is the average driving rate and τ_d is the dead time. Curves are for a Poisson process where the rate is constant (dashed curve) and for an SNDP with rectangular impulse-response function (solid curves). The dependence of the counting efficiency on the parameter $c = \mu\tau_c$ is indicated. The curves extend only up to their range of validity for $\alpha = 5$. It is clear that the efficiency is significantly reduced below the constant rate result by bunching in the SNDP. The results are analogous to those presented in Fig. 1 of [5] for a rate that is a known function of time, and in Fig. 1 of [4] for chaotic radiation.

$$\phi(y) = \sum_{k=0}^{\infty} \sum_{l=0}^{k} \sum_{m=0}^{l} \sum_{j=0}^{k-l} \cdot \frac{(-1)^j c^{k-l-j+2} [\gamma(l+j+1, y) - \gamma(l+j+2, y)/\Gamma c]}{(k-l-j)!(l-m)!m!j![c+(k-l+m)\bar{\lambda}\tau_d][c+(k-m)\bar{\lambda}\tau_d]} \tag{31}$$

where $\gamma(n,x)$ is the incomplete gamma function determined by the recurrence relation

$$\gamma(n+1,x) = n\gamma(n,x) - x^n e^{-x}, \qquad \gamma(1,x) = 1 - e^{-x}. \tag{32}$$

The quantity $\bar{\lambda}T$ is not an independent parameter since it can be written as $\alpha c\Gamma$.

In Fig. 2 we present a plot of the theoretical SNDP counting efficiency ϵ_m, which is the normalized mean $E(n)/\bar{\lambda}T$, as a function of the dead-time parameter $\bar{\lambda}\tau_d$. This quantity depends only on $\bar{\lambda}\tau_d$ and $c = \mu\tau_c$, the number of primary events per correlation time, as is evident from (25) and (28). The theory is valid only when $\bar{\lambda}\tau_d \ll \bar{\lambda}\tau_c = \alpha c$, however [see (3)]. The solid curves display the c dependence. The curves extend only up to their range of validity, e.g., the $c = 0.1$ curve is limited to $\bar{\lambda}\tau_d < 0.1$ for $\alpha = 5$. The dashed curve is the result for a Poisson point process with constant rate [$\epsilon_m \approx (1 + \bar{\lambda}\tau_d)^{-1}$; see (17)]. The solid curves lie everywhere below the dashed curve, in accordance with the upper limit on dead-time counter efficiency derived in Section 6 of [5]. For a given value of $\bar{\lambda}\tau_d = \mu\alpha\tau_d$, with μ, α, τ_d, and T all fixed, increasing c corresponds to increasing τ_c. This means that the time between correlated events increases with c. In the limit where this time becomes much greater than the dead time, the behavior should approach the Poisson result, as indeed it does. The dependence of ϵ_m on α can be understood as follows. For a given unmodified mean $\bar{\lambda}T = \mu\alpha T$, with T, τ_c, and τ_d fixed, increasing α requires a decrease in μ and therefore a decrease in c. Thus, when the multiplication parameter is increased, the counting efficiency is correspondingly reduced. This reflects the fact that a dead time kills highly bunched events more effectively than relatively unbunched events. In the limit where $\alpha \to 0$, with the unmodified mean fixed, μ (and therefore c) becomes very large and the counting efficiency approaches the Poisson result, as it should [1], [2], [8].

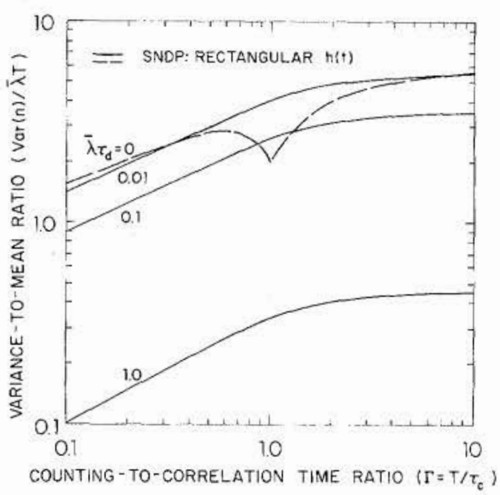

Fig. 3. Ratio of count variance to unmodified mean count, Var $(n)/\bar{\lambda}T$ versus $\Gamma = T/\tau_c$. Dashed curve is representative of an SNDP with rectangular impulse-response function in the absence of dead time ($\alpha = 5$, $c = 1$) whereas solid curves are for varying values of the dead-time parameter $\bar{\lambda}\tau_d$ as indicated. The parametric variation in the dead-time parameter is limited to $\bar{\lambda}\tau_d \ll \alpha c$ or $\bar{\lambda}\tau_d \leqslant 1.0$. It is evident that dead time generally results in a significant reduction of the variance-to-mean ratio. An anomalous region where the variance-to-mean ratio is increased by dead time appears in the vicinity of $\Gamma = 1$ for small dead time (see text). The results are equivalent to those presented in Fig. 2 of [5] for a rate that is a known function of time and in Fig. 2 of [4] for chaotic radiation.

The results presented in Fig. 2 are analogous to those presented in Fig. 1 of [5] for a rate that is a known function of time, and in Fig. 1 of [4] for chaotic radiation. The dead-time-modified count mean for chaotic light is independent of the spectrum and has no parametric dependence on a quantity analogous to c because in that case the single-fold moment-generating function $Q_{\lambda(t)}(s)$ depends only on the mean rate $\bar{\lambda}$. Equation (20) for the SNDP, on the other hand, depends on the spectrum of the shot-noise light [through the impulse response function $h(t)$], since this latter quantity is specifically linked to the occurrence of a pulse and therefore to the dead time. Equation (20), furthermore, depends on two parameters (c and β) and therefore exhibits a parametric variation.

In the absence of dead time, the SNDP count variance has been studied in detail both for rectangular and exponential $h(t)$ [1] and for arbitrary $h(t)$ [2]. It is always proportional to $\bar{\lambda}T$, unlike the count variance for chaotic light which also has a component proportional to $(\bar{\lambda}T)^2$. But like chaotic light, the unmodified count variance depends on both the first- and second-order statistics of the rate through the degrees-of-freedom parameter. It is clear that the dead-time-modified count variance also depends on the first- and second-order statistics of the rate [see (2) and (12)]. In Fig. 3 we present the ratio of the count variance to the unmodified mean, Var $(n)/\bar{\lambda}T$, versus $\Gamma = T/\tau_c$, for rectangular $h(t)$. The dashed curve shows the result in the absence of dead time, whereas

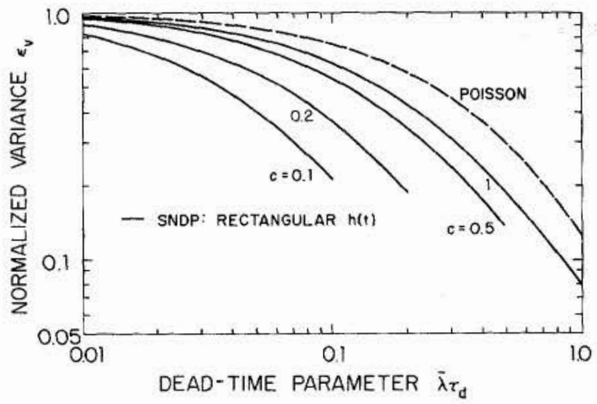

Fig. 4. Normalized variance (ratio of dead-time-modified variance to unmodified variance) ϵ_v versus $\bar{\lambda}\tau_d$, where $\bar{\lambda} = \mu\alpha$ is the average driving rate and τ_d is the dead time. Curves are for a Poisson process where the rate is constant (dashed curve) and for an SNDP with rectangular impulse-response function (solid curves). The dependence of the normalized variance on the parameter $c = \mu\tau_c$ is indicated. Curves shown are for $\alpha = 5$ and $\Gamma = 10$, but are relatively independent of these parameters (see Figs. 5 and 6). The curves extend only up to their range of validity for $\alpha = 5$. It is clear that the normalized variance is significantly reduced below the constant rate result by bunching in the SNDP. It is seen that the dependence of ϵ_v is similar to that for ϵ_m presented in Fig. 2. The results are analogous to those presented in Fig. 3 of [4] for chaotic radiation.

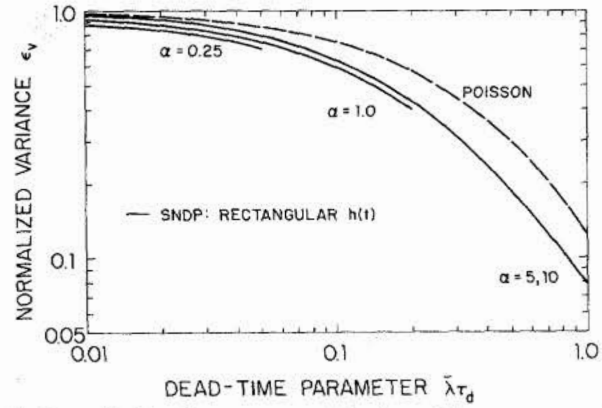

Fig. 5. Normalized variance ϵ_v versus $\bar{\lambda}\tau_d$ for a Poisson process where the rate is constant (dashed curve) and for an SNDP with rectangular impulse-response function (solid curves). The dependence of ϵ_v on the parameter α is shown to be slight ($c = 1$, $\Gamma = 10$). The curves extend only up to their region of validity for the value of α specified. Observe that the unmodified mean $\bar{\lambda}T = \mu\alpha T$ is not fixed as α is varied, but rather is proportional to α.

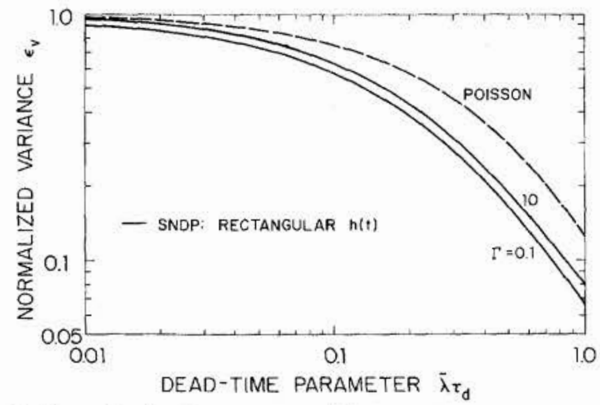

Fig. 6. Normalized variance ϵ_v versus $\bar{\lambda}\tau_d$ for a Poisson process where the rate is constant (dashed curve) and for an SNDP with rectangular impulse-response function (solid curves). The dependence of ϵ_v on the parameter Γ is shown to be slight in the extreme cases $\Gamma \ll 1$ and $\Gamma \gg 1$ ($c = 1$, $\alpha = 5$).

the solid curves represent the presence of dead time with $\bar{\lambda}\tau_d$ as a parameter. The dead-time-modified variance depends on Γ, $\bar{\lambda}\tau_d$, c, and α. As a representative example we have chosen $c = 1$ and $\alpha = 5$ (the character of the results turns out to be quite independent of these parameters though the validity of the curves requires that $\bar{\lambda}\tau_d$ and $c\alpha$ obey certain constraints as indicated earlier). By and large, the introduction of dead time produces a decrease in the variance-to-mean ratio. This is expected because dead time regularizes the pulse train. For values of $\bar{\lambda}\tau_d$ that are not too large ($\bar{\lambda}\tau_d \lesssim 0.2$), however, an interesting effect occurs in the region $\Gamma \approx 1$: the dead-time-modified variance turns out to be larger than the unmodified variance. We have previously noted that, for the rectangular impulse-response function in the absence of dead time, the unmodified variance-to-mean ratio undergoes a resonant-like reduction to a value of 2 at $\Gamma = 1$, regardless of the values of α and c [1]. We expect that this arises from the mathematically ideal nature of the rectangular filter, and we attribute the anomalous relationship of the modified and unmodified variances to a cancellation of this resonant-like reduction. Though the form of presentation is somewhat different, the information contained in Fig. 3 is similar to that conveyed by Fig. 2 of [5] for a rate that is a known function of time and by Fig. 2 of [4] for chaotic light.

In Figs. 4–6 we present the theoretical SNDP normalized count variance ϵ_v as a function of the dead-time parameter $\bar{\lambda}\tau_d$. This quantity depends on $\bar{\lambda}\tau_d$, c, α, and Γ. The dependence on c is indicated by the solid curves in Fig. 4 ($\alpha = 5$, $\Gamma = 10$), the dependence on α is shown by the solid curves in Fig. 5 ($c = 1$, $\Gamma = 10$), and the dependence on Γ is shown by the solid curves in Fig. 6 ($c = 1$, $\alpha = 5$). In all cases the curves extend only up to their range of validity, such that $\bar{\lambda}\tau_d \ll \alpha c$. It is evident from these plots that the dependence of ϵ_v on c is substantial, whereas the dependence on α and Γ is small and, to first approximation, may be disregarded. The dashed curve is the result for a Poisson process with constant rate [$\epsilon_v \approx (1 + \bar{\lambda}\tau_d)^{-3}$; see (18)].

The principal dependence of ϵ_v is on $\bar{\lambda}\tau_d$ and $c = \mu\tau_c$, as is the case for the normalized count mean ϵ_m (see Fig. 2). Again, for a given value of $\bar{\lambda}\tau_d = \mu\alpha\tau_d$, with μ, α, τ_d, and T all fixed, increasing c corresponds to increasing τ_c. This means that the time between correlated events increases with c. In the limit where this time becomes much greater than the dead time, the behavior should approach the Poisson result, as indeed it does (see Fig. 4). The dependence of ϵ_v on α can be understood as follows. For a given unmodified mean $\bar{\lambda}T = \mu\alpha T$, with T, τ_c, and τ_d fixed, increasing α requires a decrease in μ and therefore a decrease in c. Thus the normalized mean and normalized variance are both substantially reduced by an increase in α when the unmodified mean is constrained to be constant. Similarly, when $\alpha \to 0$ both ϵ_m and ϵ_v approach the Poisson result, as expected. When α is varied and the unmodified mean is not constrained to be constant, the relative independence of ϵ_v on α, illustrated in Fig. 5, emerges. The insensitivity of ϵ_v to variations in Γ, for $\Gamma \ll 1$ and $\Gamma \gg 1$, is illustrated in

Fig. 6. The curve for $\Gamma \approx 1$ lies everywhere just *above* the curve for $\Gamma = 10$.

The results presented in Fig. 4 are analogous to those presented in Fig. 3 of [4] for chaotic radiation. As in that case, the dead-time-modified count variance depends on both the first- and second-order statistics of the rate process. Because of computational complexity, we have restricted our study in this paper to a rectangular impulse-response function $h(t)$, corresponding to only a single spectral character in the chaotic case. As pointed out earlier, the quantity ϵ_v depends on the spectrum. In contradistinction, the normalized variance for chaotic light is virtually spectrum independent and, furthermore, displays no parametric dependence on a quantity analogous to c, since the multiplication degree of freedom is absent.

In the next section we proceed to a discussion of the full photon-counting distribution for radioluminescence radiation in the presence of dead time, when the counting time T is much greater than the correlation time τ_c. We then return to an experimental verification of the theoretical results for the counting efficiency ϵ_m and the normalized variance ϵ_v presented above.

IV. Photon-Counting Experiments for the SNDP in the Presence of Dead Time

We have conducted a series of experiments in which a beam of β^- particles directly irradiated the Hamamatsu UV-grade 1.55 mm thick fused-silica faceplate of an EMR Type 541N-06-14 photomultiplier tube, producing radioluminescence radiation. The high-energy electrons were generated by the Dynamitron steady-state electron accelerator at the Jet Propulsion Laboratory in Pasadena. The energy of each electron in the monoenergetic beam was about 2.2 MeV, and the emitted β^- flux was $\sim 1 \times 10^8$ cm$^{-2} \cdot$ s^{-1}. The beam emerged through a 2 mil thick titanium foil window. It traveled a distance of about 1.5 m, to a 0.6 cm diameter hole in a lead brick, covered with a thin aluminum plate containing a small aperture. The sample was located behind the hole. The estimated flux at the faceplate of the photomultiplier tube was 10^5 s^{-1}. The quantum efficiency was about 18 percent at 4000 Å. External light was excluded. The photomultiplier anode pulses were passed through a discriminator and standardized (EMR Type 617K-11-M4). An external electronic circuit enabled the point process to be modified by an adjustable constant nonparalyzable dead time τ_d; the minimum value of τ_d (60 ns) was limited by the discriminator and standardizing electronics. The surviving pulses were counted during consecutive fixed counting intervals ($T = 400$ μs) and the counts were recorded. The experiment was performed repeatedly to obtain good statistical accuracy and a histogram representing the relative frequency of the counts was constructed. This procedure was carried out for various values of the dead time τ_d; in each case the count mean and variance were computed from the experimental histogram. The duration of a run was about 10 s.

In the first experiment that we illustrate, the observed mean count was 119.25 (this number was substantially higher than the mean dark count which could therefore be neglected) and the observed count variance was 1220.0 when the adjustable dead time was set at its minimum value of 60 ns. The data are shown as the solid dots in Fig. 7. The solid curve represents the Neyman Type-A theoretical counting distribution with the count mean and variance fixed at the experimental values. It is clearly in accord with the data; we have also previously shown this for Sr^{90}-Y^{90}-induced radioluminescence radiation in glass [2]. Assuming that $\tau_c \ll T$ (1 mode, $\mathfrak{M} = 1$), and assuming also that the effects of this minimum dead time are negligible, the experimental multiplication parameter $\alpha = [\mathrm{Var}(n)]/E(n) - 1 = 9.2$ [2, eq. (13)]. Actually, because the primary process in this case consisted of high-energy charged particles (electrons), Čerenkov radiation was probably produced in addition to luminescence radiation. However, even if a large number of photoelectrons were generated by the Čerenkov photons arising from a single particle, they would nevertheless appear as a single (large) photoelectron pulse, since the Čerenkov radiation emission time is much shorter than the transit time in the photomultiplier tube [8].

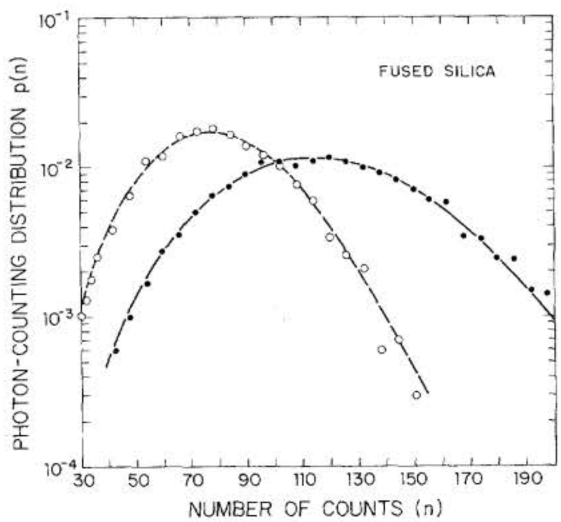

Fig. 7. Photon-counting distribution $p(n)$ versus number of photon counts n. Data (solid dots) represent radioluminescence photon registrations induced in the fused-silica faceplate of the EMR photomultiplier tube by high-energy β^- rays, when the dead time τ_d is small (60 ns). The counting time $T = 400$ μs. The experimental count mean and variance are 119.25 and 1220.0, respectively. The solid curve represents the Neyman Type-A theoretical counting distribution with the same values of count mean and variance ($\alpha = 9.2$). Open dots represent experimental data for $\tau_d = 200$ ns. The dashed curve is the Neyman Type-A with a mean and variance set equal to the experimental values.

The open circles in Fig. 7 represent the relative frequencies of the counts at an increased level of dead time, $\tau_d = 200$ ns. In this case, the observed mean count and the count variance were 80.66 and 554.0, respectively. The dashed curve represents a Neyman Type-A theoretical counting distribution with the count mean and variance fixed at these experimental values. The fit is very good. Although the only general theory available for the dead-time-modified SNDP photon-counting distribution is limited by the restriction $T \ll \tau_c$ (see [9], [10]), a simple physical argument demonstrates that the Neyman Type-A provides an appropriate theoretical choice in the case of our experiments.

The argument begins with Fig. 8, which is a plot of the observed dead-time-modified mean count $E(n)$ versus the count variance-to-mean ratio $\mathrm{Var}(n)/E(n)$ for the three transparent materials. The dead time is varied parametrically so that the

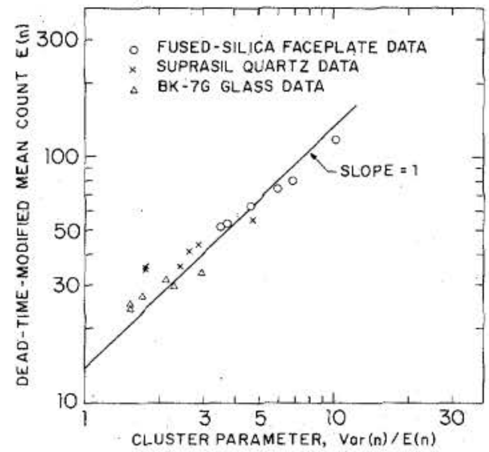

Fig. 8. Dead-time-modified mean count $E(n)$ versus cluster parameter [$\mathrm{Var}(n)/E(n)$] for β^--induced radioluminescence radiation from three transparent materials [fused-silica faceplate of EMR photomultiplier tube (○), suprasil quartz (×), and BK-7G Cr-doped Schott glass (△)]. The six experimental points for each material represent different values of the fixed nonparalyzable dead time (τ_d = 60, 200, 400, 600, 800 ns, 1 μs). The data are seen to lie along a line of unity slope on this log–log plot.

six experimental points for each material represent different values of the fixed nonparalyzable dead time (τ_d = 60, 200, 400, 600, 800 ns, 1 μs). The variance-to-mean ratio plotted on the abscissa may be viewed as excess clustering above the Poisson [for which $\mathrm{Var}(n)/E(n) = 1$]. The data for all materials are seen to lie along a straight line of unity slope on this log–log plot. This indicates that the reduction in mean count produced by increasing the dead time is associated with a decrease in the excess clustering. When c is small, secondary events belonging to different clusters are well separated and the dead time simply reduces the effective multiplication parameter and the mean count by approximately the same quantity. The distribution therefore maintains its Neyman Type-A character.

This interpretation is consistent with the parameters relevant to our experiment. In Section V we will see that for the materials we have studied, $c = \mu\tau_c \simeq 0.2$ with $\tau_c \simeq 5$ μs and $\mu^{-1} \simeq$ 25 μs. Recalling that τ_c is the time over which secondary events are clustered and μ^{-1} is the average primary interarrival time, values of $\tau_d \lesssim 5$ μs will kill an increasing number of secondaries as the dead time is increased (always leaving the first secondary event that triggered the dead time intact, of course). Thus, it is expected that under the conditions of our experiment ($c \ll 1$, $\mu\tau_d \ll 1$, $T \gg \tau_c$) the dead-time-modified counting distribution will be well represented by the Neyman Type-A with a reduced mean and variance. When τ_d becomes somewhat larger than τ_c, with the conditions $c \ll 1$, $\mu\tau_d \ll 1$, and $T \gg \tau_c$ maintained, only a single secondary pulse will remain per cluster, and the counting distribution will approach the Poisson. It will then remain Poisson until τ_d increases to the point that it begins to kill events associated with other clusters ($\mu\tau_d \sim 1$). If Čerenkov radiation is present, primary events will also be registered and it is these that will trigger the dead time; but in any case the behavior will be very similar to that described above.

Additional experimental photon-counting distributions are presented in Figs. 9 and 10. In this case the β^- particle beam

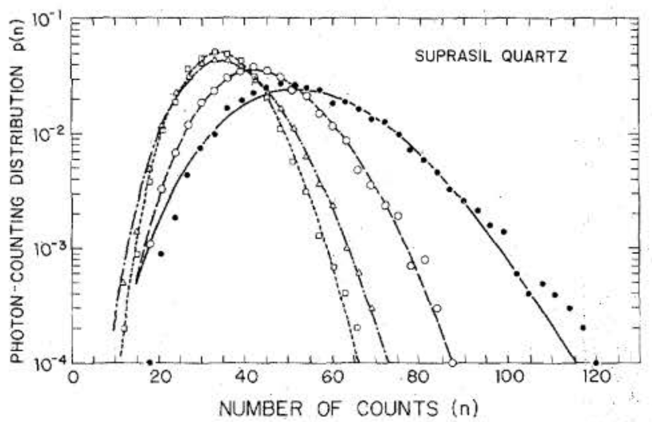

Fig. 9. Photon-counting distribution $p(n)$ versus number of photon counts n. Data (solid dots) represent radioluminescence photon registrations induced in suprasil quartz by high-energy β^- rays, when the dead time is small (60 ns). The counting time $T = 400$ μs. The experimental count mean and variance are 55.01 and 260.6, respectively. The solid curve represents the Neyman Type-A theoretical counting distribution with the same values of count mean and variance ($\alpha = 3.73$). Open symbols represent experimental data for increasing values of τ_d (200 ns, ○; 600 ns, △; 1 μs, □). The broken curves represent Neyman Type-A distributions with mean and variance values chosen in accordance with the experimental data.

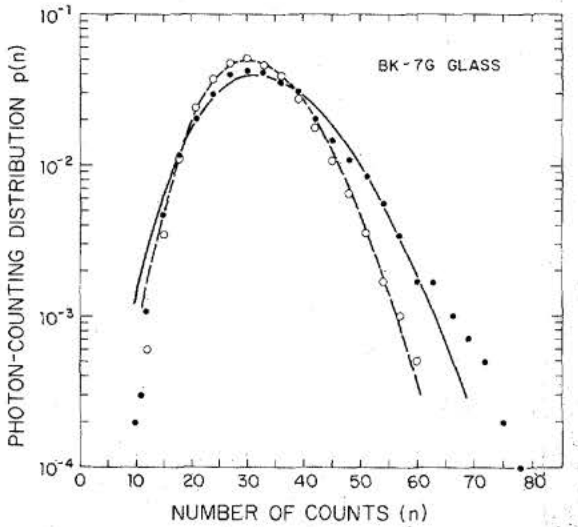

Fig. 10. Photon-counting distribution $p(n)$ versus number of photon counts n. Data (solid dots) represent radioluminescence photon registrations induced in BK-7G Cr-doped Schott glass by high-energy β^- rays, when the dead time is small (60 ns). The counting time T = 400 μs. The experimental count mean and variance are 33.59 and 99.53, respectively. The solid curve represents the Neyman Type-A theoretical counting distribution with the same values of count mean and variance ($\alpha = 1.96$). Open dots represent experimental data for τ_d = 200 ns. The dashed curve is the Neyman Type-A with a mean and variance set equal to the experimental values.

impinged on external samples of Amversil suprasil quartz and BK-7G Cr-doped Schott glass, respectively. The optical radiation then entered the photomultiplier tube and a photon-counting experiment was performed. Nominal values for the mean, variance, and α parameters are 55.01, 260.6, and 3.73, respectively, for Fig. 9 and 33.59, 99.53, and 1.96, respectively, for Fig. 10 when the dead time took on its minimum value (solid dots). The Neyman Type-A theoretical counting distribution provides an excellent fit to the data in all cases, both in the absence and in the presence of dead time. Indeed it is conceivable that the 60 ns nominal dead time associated with

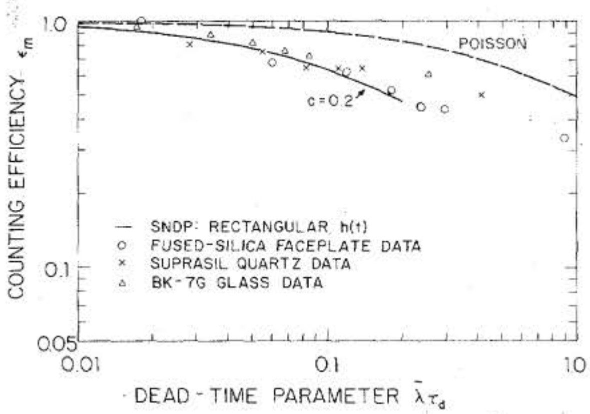

Fig. 11. Experimental counting efficiency ϵ_m versus $\overline{\lambda}\tau_d$ for radioluminescence photon counts generated in the fused-silica faceplate of the EMR photomultiplier tube (○), in suprasil quartz (×), and in BK-7G Cr-doped Schott glass (△). The radioluminescence was induced by high-energy β^- rays. The three sets of experimental data are in good accord with the theoretical result expected for an SNDP with rectangular impulse-response function and $c = 0.2$ as shown (solid curve). The theoretical curve extends only up to its range of validity for $\alpha = 5$. The dashed curve is the result for a Poisson process where the rate is constant.

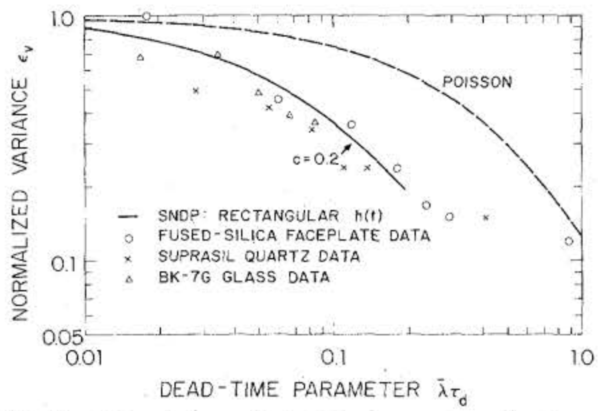

Fig. 12. Experimental normalized variance ϵ_v versus $\overline{\lambda}\tau_d$ for radioluminescence photon counts generated in the fused-silica faceplate of the EMR photomultiplier tube (○), in suprasil quartz (×), and in BK-7G Cr-doped Schott glass (△). The radioluminescence was induced by high-energy β^- rays. The three sets of experimental data are in good accord with the theoretical result expected for an SNDP with rectangular impulse-response function and $c = 0.2$ as shown (solid curve). Though the solid curve has been generated assuming $\alpha = 5$ and $\Gamma = 10$, it is principally sensitive only to the value of c, as is illustrated in Figs. 4–6. The best-fitting value of c for the counting efficiency ϵ_m is also 0.2 (see Fig. 11). The theoretical curve extends only up to its range of validity for $\alpha = 5$. The dashed curve is the result for a Poisson process where the rate is constant.

the electronics has killed some events without our knowledge, and that the constancy of the Neyman Type-A has already come into play in the data fit by the solid curves.

Finally, we note that the experimental dead-time-modified photon-counting distribution produced in 7056 glass (not displayed here), for example, shows evidence of scallops, whereas the associated Neyman Type-A theoretical photon-counting distribution does not. This may reflect behavior more like the fixed multiplicative Poisson [8], possibly indicating that the number of primaries, or the number of secondaries per primary, is confined to a range narrower than the Poisson.

V. Experimental Dead-Time-Modified Count Mean and Variance for the SNDP

In the photon-counting experiments described in the previous section, the count mean and variance were monitored as the fixed dead time was varied over a broad range. This enabled us to obtain three sets of experimental data for both the counting efficiency ϵ_m and the normalized variance ϵ_v as a function of $\overline{\lambda}\tau_d$. The results for ϵ_m are presented in Fig. 11 for radiation generated in the fused-silica faceplate of the EMR photomultiplier tube (○), by an external sample of suprasil quartz (×), and by an external sample of BK-7G Cr-doped Scott glass (△). Analogous results for ϵ_v are presented in Fig. 12.

It is evident from the solid curves in Figs. 11 and 12 that all of the experimental data are in good accord with the theoretically predicted result for an SNDP, with rectangular impulse-response function, and $c = 0.2$ (see Figs. 2 and 4). Though the curve for ϵ_v has been generated using the specific values $\alpha = 5$ and $\Gamma = 10$, it is principally sensitive only to the value of c, as illustrated in Figs. 4–6. The theoretical curves extend only up to their range of validity for $\alpha = 5$. The dashed curves in Figs. 11 and 12 represent the theoretical results for a Poisson process where the rate is constant. The experimental efficiency and normalized variance are both significantly reduced below the constant rate result by bunching in the SNDP, as emphasized earlier.

Using the extracted value for c, together with the values of α for nominal dead time reported in the previous section, and assuming μ constant, we can extract values of τ_c for the various cases. The appropriate relationships are $\overline{\lambda} = \mu\alpha$ and $c = \mu\tau_c$. Eliminating μ we find $\tau_c = \alpha c/\overline{\lambda}$. But since $\overline{\lambda} = E(n)/T$, $\tau_c = \alpha c T/E(n)$. Substituting $c = 0.2$, $T = 400$ μs, and the appropriate values of α and $E(n)$ for each material, we find τ_c (fused silica) $\simeq 6.2$ μs, τ_c(suprasil) $\simeq 5.4$ μs, and τ_c(BK-7G) $\simeq 4.7$ μs. This justifies the assumption that $T \gg \tau_c$. The calculated value for μ is therefore $\simeq 4 \times 10^4$ s^{-1}, which is in good accord with the estimated flux at the material and with the extrapolated value of μT obtained from Fig. 8 [at Var $(n)/E(n) = 1$].

VI. Conclusion

We have shown that the dead-time-modified count mean and variance for an arbitrary DSPP can be obtained from the Laplace transform of the single-fold and joint moment-generating functions for the driving rate process. The result is valid for an arbitrary sampling time, when the (nonparalyzable) dead time is small in comparison with the correlation time of the driving rate process.

We have applied the results to the SNDP and obtained analytical expressions for the dead-time-modified count mean and variance when the impulse-response function $h(t)$ is rectangular. The counting efficiency ϵ_m and the normalized variance ϵ_v have been graphically presented as a function of the dead-time parameter $\overline{\lambda}\tau_d$. The former, ϵ_m, has been shown to depend only on the number of primary events per correlation time $c = \mu\tau_c$ whereas ϵ_v has been shown to depend principally on c, and only slightly on α and Γ. The results have been compared with those obtained previously for chaotic light. We have not carried out explicit calculations for impulse-response functions other than rectangular because of the algebraic complexity of the expressions. Since $\tau_d \ll \tau_c$, we speculate that the character of the dead-time-modified mean and variance do not depend substantially on the specific choice of $h(t)$, however.

Photon-counting experiments were conducted with radioluminescence radiation from three transparent materials. Both the dead-time-modified photon-counting distribution and the count mean and variance were measured as the dead time τ_d was varied over a broad range. The experimental counting efficiency and normalized variance were shown to be well fit by the theoretical curves for an SNDP with rectangular impulse-response function. As expected, both ϵ_m and ϵ_v were significantly reduced below the constant-rate Poisson result by clustering in the SNDP. Values for the parameters μ, α, and τ_c were extracted for each material. Because the natural impulse-response function for the materials studied was likely exponential rather than rectangular, the satisfactory fit of our theory to experiment, together with the internal consistency of the extracted parameter values, provides support for the notion that ϵ_m and ϵ_v do not depend critically on $h(t)$ in the small dead-time limit.

We have already emphasized that the results presented here are valid only for small τ_d [see (3) and (4)]. As τ_d becomes larger, the functional form of $h(t)$ is expected to increasingly affect both $E(n)$ and $\mathrm{Var}(n)$. Indeed, the shape of $h(t)$ should play a substantial role as τ_d approaches τ_c. A form of dead-time spectroscopy using the mean count, analogous to that discussed previously for chaotic light [4], may therefore be possible. In fact, for $\mu\tau_c \ll 1$ (well-separated clusters), with α large and $\mu\tau_d \ll 1$ (which restricts the dead time to individual clusters), quite a lot of information about the form of $h(t)$ may be inferred by examining the count mean and variance as τ_d is varied from $\ll\tau_c$ to $\gg\tau_c$. Furthermore, it can be intuitively argued that, in the context of fixed dead-time signal processing, the separation of an SNDP from a Poisson point process (or from another point process that is bunched or antibunched in a distinctive way) may sometimes be best achieved by choosing $\tau_d \gtrsim \tau_c$. This is especially easy to see if the clusters are well separated and if the SNDP represents an undesirable noise process. The use of dead time in signal processing applications [11], [12] is one of the primary motivations in carrying out this study.

Thus, an analysis of the count mean and variance in the regime $\tau_d \gtrsim \tau_c$, though difficult to carry out, may be quite useful. The experimental data in Figs. 11 and 12 are seen to diverge from an extrapolation of the present theory when the condition $\tau_d \ll \tau_c$ is not obeyed. One can begin to see what happens. As $\bar{\lambda}\tau_d$ nears 1, τ_d becomes comparable with τ_c. Since $c = 0.2 \ll 1$, $\mu\tau_d \approx \mu\tau_c \ll 1$; thus the clusters are well separated and the occurrence of a dead time kills only secondary pulses associated with a given cluster. Now if τ_d were made somewhat larger than τ_c, all secondaries save one per cluster (the initiator of the dead time) would be killed, ideally leaving a Poisson point process of rate μ. Any further increase in the dead time would then have no effect on the point process until it becomes sufficiently large ($\mu\tau_d \sim 1$) to kill secondary events associated with other clusters. The data in Figs. 11 and 12, though sparse in this region, provide some evidence for an independence of the count mean and variance on $\bar{\lambda}\tau_d$ as this quantity approaches 1.

Experimental photon-counting distributions for the three transparent materials are well described by the Neyman Type-A distribution over a broad range of dead times (60 ns–1 μs, $\tau_d \ll \tau_c$). Although the only general theory available for the dead-time-modified DSPP counting distribution is limited by the restriction $T \ll \tau_c$ (see [9] and [10]), we have presented a plausible argument to indicate why the Neyman Type-A provides a suitable theoretical description for the SNDP we have considered ($\mu\tau_c \ll 1$, $\mu\tau_d \ll 1$, $T \gg \tau_c$). It is possible that this line of reasoning is particularly appropriate for rectangular and exponential impulse response functions. It is because of the particle-like nature of the SNDP that the theoretical situation is much better than one would imagine at first. The Neyman Type-A has recently been analyzed in substantial detail; it converges in distribution to the Gaussian [8] and has a simple approximate normalizing transform [13]. It can therefore be dealt with quite easily in the context of detection and estimation problems.

As some of the conditions specified above are relaxed, we would expect different results. For example, when $c \gg 1$ many primary events can occur within the correlation time τ_c and the dead-time-modified count mean and variance, along with the underlying point process, approach Poisson (see Figs. 2 and 4). In this case, the counting distribution (dead-time-modified Poisson) is well known [7], [9], but theoretical results are unavailable for arbitrary $\mu\tau_c$, $\mu\tau_d$, and T/τ_c.

Appendix
Proof of the Laplace Transform Relations

Consider the integrals

$$\int_0^\infty \exp(-s)\exp(-sX)\,ds = \frac{1}{1+X} = 1 - \frac{X}{1+X}, \tag{A1}$$

$$\int_0^\infty \left(s - \frac{s^2}{2}\right)\exp(-s)\exp(-sX)\,ds = \frac{1}{(1+X)^2} - \frac{1}{(1+X)^3} = \frac{X}{(1+X)^3}, \tag{A2}$$

$$\int_0^\infty\int_0^\infty \exp(-s_1 - s_2)\exp(s_1X_1 - s_2X_2)\,ds_1\,ds_2 = \frac{1}{1+X_1}\cdot\frac{1}{1+X_2} = 1 - \frac{X_1}{1+X_1} - \frac{X_2}{1+X_2} + \frac{X_1X_2}{(1+X_2)(1+X_2)}. \tag{A3}$$

Forming the expectation values of both sides of each equation and organizing terms, we have

$$\left\langle\frac{X}{1+X}\right\rangle = 1 - \int_0^\infty Q_X(s)\,e^{-s}\,ds \tag{A4}$$

$$\left\langle\frac{X}{(1+X)^3}\right\rangle = \int_0^\infty Q_X(s)\left(s - \frac{s^2}{2}\right)e^{-s}\,ds \tag{A5}$$

$$\left\langle\frac{X_1}{1+X_1}\cdot\frac{X_2}{1+X_2}\right\rangle = 1 - 2\int_0^\infty Q_X(s)\,e^{-s}\,ds + \int_0^\infty\int_0^\infty Q_{X_1,X_2}(s_1,s_2)\cdot e^{-s_1-s_2}\,ds_1\,ds_2. \tag{A6}$$

Using (7) and (10), (5), (6), and (9) directly follow.

ACKNOWLEDGMENT

We are grateful to M. Birnbaum and R. Bunker of the Jet Propulsion Laboratory for many valuable discussions and for providing us with access to the JPL Dynamitron, where these measurements were carried out.

REFERENCES

[1] B.E.A. Saleh and M. C. Teich, "Multiplied-Poisson noise in pulse, particle, and photon detection," *Proc. IEEE*, 1982, to be published.

[2] M. C. Teich and B.E.A. Saleh, "Fluctuation properties of multiplied-Poisson light: Measurement of the photon-counting distribution for radioluminescence radiation from glass," *Phys. Rev. A*, vol. 24, pp. 1651–1654, 1981.

[3] —, "Interevent-time statistics for shot-noise-driven self-exciting point processes in photon detection," *J. Opt. Soc. Amer.*, vol. 71, pp. 771–776, 1981.

[4] G. Vannucci and M. C. Teich, "Dead-time-modified photocount mean and variance for chaotic radiation," *J. Opt. Soc. Amer.*, vol. 71, pp. 164–170, 1981.

[5] —, "Effects of rate variation on the counting statistics of dead-time-modified Poisson processes," *Opt. Commun.*, vol. 25, pp. 267–272, 1978.

[6] E. Parzen, *Stochastic Processes*. San Francisco: Holden-Day, 1962.

[7] J. W. Müller, "Some formulae for a dead-time-distorted Poisson process," *Nucl. Instr. Methods*, vol. 117, pp. 401–404, 1974.

[8] M. C. Teich, "Role of the doubly stochastic Neyman Type-A and Thomas counting distributions in photon detection," *Appl. Opt.*, vol. 20, pp. 2457–2467, 1981.

[9] B. I. Cantor and M. C. Teich, "Dead-time-corrected photocounting distributions for laser radiation," *J. Opt. Soc. Amer.*, vol. 65, pp. 786–791, 1975.

[10] M. C. Teich and G. Vannucci, "Observation of dead-time-modified photocounting distributions for modulated laser radiation," *J. Opt. Soc. Amer.*, vol. 68, pp. 1338–1342, 1978.

[11] M. C. Teich and B. I. Cantor, "Information, error, and imaging in deadtime-perturbed doubly stochastic Poisson counting systems," *IEEE J. Quantum Electron.*, vol. QE-14, pp. 993–1003, 1978.

[12] G. Vannucci and M. C. Teich, "Equivalence of threshold detection with and without dead time," *Appl. Opt.*, vol. 18, pp. 3886–3887, 1979.

[13] P. R. Prucnal and M. C. Teich, "Multiplication noise in the human visual system at threshold: 2. Probit estimation of parameters," *Biol. Cybern.*, 1981, to be published.

Bahaa E. A. Saleh (M'73) received the B.S. degree from Cairo University, Cairo, Egypt, in 1966, and the Ph.D. degree from Johns Hopkins University, Baltimore, MD, in 1971, both in electrical engineering.

From 1971 to 1974 he was an Assistant Professor at the University of Santa Catarina, Brazil. Thereafter, he joined the Max-Planck Institute, Göttingen, Germany, where he was involved in research in laser light scattering and photon correlation spectroscopy. In 1976 he was a Visiting Professor at the University of Kuwait, and in 1977 a Visiting Research Associate with the Physiological Optics Group at the School of Optometry, University of California, Berkeley. He is presently a Professor of Electrical and Computer Engineering at the University of Wisconsin, Madison, where he has been since 1977.

He is currently involved in research in image processing, optical data processing, optical communication, and vision.

Dr. Saleh is the author of *Photoelectron Statistics* (Berlin: Springer, 1978). He is a member of Phi Beta Kappa, Sigma Xi, the Optical Society of America, and the Society of Photo-Optical Instrumentation Engineers. He is an Associate Editor of the *Journal of the Optical Society of America*.

Joseph T. Tavolacci (S'58–M'62–M'78) was born in New York City, NY, on August 4, 1939. He attended Manhattan College, New York, NY, on a New York State Regents Scholarship and received the B.E.E. degree in 1961. He has done graduate study at Fairleigh Dickinson University, Rutherford, NJ, and at the University of Colorado, Boulder.

In 1961, he joined the Kollsman Instrument Corporation and performed design and development work in the Advanced Star-Tracking Group, with emphasis on all-electronic strap-down systems. In 1965, he accepted a position at the Bendix Corporation, Teterboro, NJ, and participated in the OAO Gimballed Star-Tracker Program with responsibilities for the detector subcontract and qualification testing of the system. He was then assigned to the Skylab Program in Denver for five years. While on this program, his tasks included interface definition for the Apollo Telescope Mount experiments and test requirement definition for the Skylab attitude-control subsystems. He returned to Teterboro in 1972 and conducted development and test activities of vertical-scale instruments for the B-1 program. Since 1973 he has been a member of the Electro-Optics Group in the Guidance Systems Division performing design, test, and analysis work in the area of star scanners. His most recent assignment is as Technical Manager of the Star-Scanner Program for the NASA/JPL Galileo Orbiter Mission.

Malvin Carl Teich (S'62–M'66–SM'72) was born on May 4, 1939, in New York City, NY. He received the S.B. degree in physics from the Massachusetts Institute of Technology, Cambridge, MA, in 1961, the M.S. degree in electrical engineering from Stanford University, Stanford, CA, in 1962, and the Ph.D. degree in quantum electronics from Cornell University, Ithaca, NY, in 1966. While at M.I.T. he received the Frank W. and Carl S. Adams Memorial Scholarship, and at Cornell University he received the James Clerk Maxwell Fellowship and a Ford Foundation Grant.

He has held summer research positions at the Motorola Corporation, Rockwell International's Space and Information Systems Division, and the Mitre Corporation in 1959, 1961, and 1963, respectively. In the summer of 1960 he participated in a Student Technical Exchange Program at N.V. Philips Gloeilampenfabrieken, Eindhoven, The Netherlands. In 1966 he joined the M.I.T. Lincoln Laboratory, Lexington, MA, where he was engaged in work on coherent infrared detection and modulation. In 1967, he became a member of the faculty in the Department of Electrical Engineering, Columbia University, New York, NY, where he is now teaching and pursuing his research interests in the areas of optical and infrared detection, lightwave communications, and sensory perception. He served as Chairman of the Department from 1978 to 1980. He is currently also a member of the faculty in the Department of Applied Physics and Nuclear Engineering, a member of the Columbia Radiation Laboratory, and a member of the Columbia Bioengineering Institute.

Dr. Teich has authored or coauthored some 80 technical publications and holds one patent. He is a member of Sigma Xi, the American Physical Society, the Optical Society of America, the Acoustical Society of America, the Society for Neuroscience, and the New York Academy of Sciences. In 1969 he was the recipient of the IEEE Browder J. Thompson Memorial Prize Award for his paper "Infrared Heterodyne Detection," and in 1973 was appointed a Fellow of the John Simon Guggenheim Memorial Foundation. He served as a member of the Editorial Advisory Panel for *Optics Letters* from 1977 to 1979.